Journal of Computational Physics 228 (2009) 2213–2224

Contents lists available at ScienceDirect

Journal of Computational Physics

journal homepage: www.elsevier.com/locate/jcp

An improved Quiet Direct Simulation method for Eulerian fluids using a second-order scheme

M.R. Smith [a,b], H.M. Cave [b,c], J.-S. Wu [b,*], M.C. Jermy [c], Y.-S. Chen [d]

[a] National Center for High Performance Computing, National Applied Research Laboratories, No. 7 R&D Rd. VI, Hsinchu Science Park, Hsinchu, Taiwan
[b] Department of Mechanical Engineering, National Chiao Tung University, 1001 Ta-Hsueh Road, Hsinchu 30050, Taiwan
[c] Department of Mechanical Engineering, University of Canterbury, Private Bag 4800, Christchurch 8140, New Zealand
[d] National Space Organization, National Applied Research Laboratories, 8F, 9 Zhan-Ye 1st Road, Hsinchu Science Park, Hsinchu, Taiwan

ARTICLE INFO

Article history:
Received 6 June 2008
Received in revised form 1 December 2008
Accepted 1 December 2008
Available online 24 December 2008

Keywords:
Quiet Direct Simulation
QDS
Euler solver
Second-order method

ABSTRACT

In this paper, a second-order scheme for the Quiet Direct Simulation (QDS) of Eulerian fluids is proposed. The QDS method replaces the random sampling method used in Direct Simulation Monte Carlo (DSMC) methods with a technique whereby particles are moved, have their properties distributed onto a mesh, are destroyed and then are recreated deterministically from the properties stored on the mesh using Gauss–Hermite quadrature weights and abscissas. Particles are permitted to move in physically realistic directions so flux exchange is not limited to cells sharing an adjacent interface as in conventional, direction decoupled finite volume solvers. In this paper the method is extended by calculating the fluxes of mass, momentum and energy between cells assuming a linear variation of density, temperature and velocity in each cell and using these fluxes to update the mass, velocity and internal energy carried by each particle. This Euler solver has several advantages including large dynamic range, no statistical scatter in the results, true direction fluxes to all nearby neighbors and is computationally inexpensive. The second-order method is found to reduce the numerical diffusion of QDS as demonstrated in several verification studies. These include unsteady shock tube flow, a two-dimensional blast wave and of the development of Mach 3 flow over a forward facing step in a wind tunnel, which are compared with previous results from the literature wherever is possible. Finally the implementation of QUIETWAVE, a rapid method of simulating blast events in urban environments, is introduced and the results of a test case are presented.

1. Introduction

The particle-based Direct Simulation Monte Carlo (DSMC) method has been arguably the most successful method for simulating rarefied gas flows since its development by Bird in the 1960s [1]. In DSMC, the flow is simulated by tracking the movement of a large number of simulated particles through the flow field. After the convection of the particles over a time step which is a fraction of the mean collision time, the particles are indexed to a grid and randomly selected to suffer scattering collisions. These collisions are generated on a probabilistic basis requiring the use of random numbers for collision partner selection and to determine the likelihood of the collision actually occurring. As such, DSMC is subject to statistical scatter and requires averaging over a large number of time steps to reduce the scatter in the sampled macroscopic properties.

* Corresponding author. Tel.: +886 3 573 1693; fax: +886 3 611 0023.
E-mail address: chongsin@faculty.nctu.edu.tw (J.-S. Wu).

0021-9991/$ - see front matter © 2008 Elsevier Inc. All rights reserved.
doi:10.1016/j.jcp.2008.12.013

In the high collision rate limit, the particle velocity distributions approach that of the Maxwell–Boltzmann equilibrium distribution and moments of the Boltzmann equation reduce to the Euler equations [2]. Several authors proposed methods in which the particles do not undergo collision events, but rather are regenerated by having their velocities drawn from the local Maxwellian. In Pullin's Equilibrium Particle Simulation Method (EPSM) [3], the standard collision phase in DSMC is replaced by a method whereby particles are assigned new velocities based on the state of the cell without having their positions changed. To ensure energy and momentum are conserved, the routine enforces identical mean and variance values of the pre- and post-collision velocity distributions. However, the technique does exhibit statistical scatter in the results and as such requires averaging over a large number of time steps in the same way as DSMC.

Pullin also proposed the Equilibrium Flux Method (EFM) in which fluxes are calculated analytically across the interface of two cells for the limit of an infinite number of particles, a very small time step and assuming uniform conditions across the cells [3]. This method has been implemented in higher dimensions by Macrossan [4]. The technique is not subject to the statistical scatter inherent in particle-based methods; however because EFM calculates the fluxes across the interfaces between cells, it is a direction decoupled method for simulations having more than one dimension. Recently Smith et al. [5] has developed the True Direction Equilibrium Flux Method (TDEFM) in which fluxes can be exchanged between all cells to which particles can flux during a time step, regardless as to whether they share an interface or not. These fluxes are calculated by integrating the Maxwell–Boltzmann distribution over both velocity-space and the cell volume in the limit of an infinite number of particles and assuming uniform conditions across the cell. TDEFM thereby eliminates the direction decoupling induced errors of EFM and other traditional finite volume solvers, and the calculated fluxes are valid for any size time step.

The Quiet Direct Simulation (QDS) method was original developed by Albright et al. [6] as a method for modeling plasmas. They subsequently applied QDS to the simulation of Eulerian fluids for Sod's one-dimensional shock tube problem and a simple two-dimensional blast wave problem. Since then little further work has been done, the only example being by Peter [7] who applied a random time step to the movement of simulation particles for simulating a typical diffusion equation. In the QDS method, the effect of sampling using random numbers is replaced by using the weights and abscissas of a Gauss–Hermite quadrature. Thus, QDS is a particle-based Euler solver which exhibits negligible statistical scatter, has a large dynamic range, is easily extended to multi-dimensions and multi-species, is computationally inexpensive, is easily implemented on parallel computers and, since it is a particle-based method, does not require direction decoupling. The major disadvantage is the scheme is inherently very diffusive. Albright et al. [6] named the technique the Quiet DSMC (QDSMC) method; however the present authors feel this is a misnomer as no there is no random number (or Monte Carlo) component to the algorithm and, unlike DSMC, it is valid only when thermal equilibrium can be assumed.

There are several advantages to particle-based Euler solvers. Firstly, hybridization between the solver and a pure DSMC solver which is capable of simulating the non-continuum regions of flow is relatively simple. Several authors have developed such particle-based hybrid methods including Macrossan [8], Chen [9], Smith [10] and Wu [11]. The second major advantage is that particle-based methods can exchange fluxes between any two cells on the grid for any given time step. Direction decoupled computational fluid dynamics (CFD) methods only allow fluxes to be exchanged between cells sharing a common interface. This physically unrealistic situation results in non-physical results in CFD simulations [5,12].

In this paper, we extend the QDS algorithm so that particle properties are updated considering the fluxes of mass, momentum and energy between cells which are generated using a second-order flux reconstruction scheme. The principles of the QDS method and the extension to a second order, two-dimensional solver are discussed. Validation simulations of one-dimensional shock flow, a two-dimensional blast wave and the high speed flow over a forward facing step are then carried out. Finally, a tool for modeling the effect of blast waves in urban environments which utilizes QDS, called QUIETWAVE, is introduced. This software can predict blast behavior in a matter of minutes using standard desktop computers.

2. Numerical method

2.1. First-order particle-based scheme

The normal random variable $N(0,1)$ is defined by the probability density:

$$p(x) = \frac{e^{-x^2/2}}{\sqrt{2\pi}} \tag{1}$$

By using a Gaussian quadrature approximation, the integral of Eq. (1) over its limits can be approximated by:

$$\int_{-\infty}^{\infty} \frac{e^{-x^2/2}}{\sqrt{2\pi}} f(x)dx \approx \sum_{j=1}^{J} \frac{w_j}{\sqrt{\pi}} f\left(\sqrt{2}q_j\right) \tag{2}$$

where w_j and q_j are the weights and abscissas of the Gaussian quadrature (also known as the Gauss–Hermite parameters). The abscissas are the roots of the Hermite polynomials which can be found tabulated in reference [13] or can be defined by the recurrence equation:

$$H_{n+1}(q) = 2qH_n - 2nH_{n-1} \tag{3}$$

where $H_{-1} = 0$ and $H_0 = 1$. The weights can be determined from:

$$w_j = \frac{2^{n-1} n! \sqrt{\pi}}{n^2 [H_{n-1}(q_i)]^2} \tag{4}$$

Eq. (2) becomes exact when the function $f(x)$ is a linear combination of the $2J-1$ polynomials $x^0, x^1, \ldots, x^{2J-1}$.

Thus the basic first-order one-dimensional QDS algorithm consists of three basic steps (the method can be readily extended to higher dimensions) [6]:

(1) Particles undergo a "quiet start". Here $j = 1, \ldots, J$ particles are generated on the grid point x_i from the known grid quantities of density (ρ_i), velocity (u_i), velocity variance (σ^2_{vi}) and energy (E_i). The particles masses, velocities and internal energies are, respectively:

$$m_{ij} = \frac{\rho_i \Delta x w_j}{\sqrt{\pi}} \tag{5}$$

$$v_{ij} = u_i + \sqrt{2\sigma^2_{vi}} q_j \tag{6}$$

$$\varepsilon_{ij} = \frac{(\xi - \Omega)\sigma^2_{vi}}{2} \tag{7}$$

where Δx is the uniform grid size, ξ is the total number of degrees of freedom ($\xi = 2(\gamma - 1)^{-1}$) and Ω is the number of simulated translation degrees of freedom (i.e. for one-dimensional simulation, $\Omega = 1$). Any unused translational and other non-translational degrees of freedom are thus treated as internal structural degrees of freedom.

(2) Particles are advanced to their new position over a time step Δt such that:

$$x_{ij}(t + \Delta t) = x_i + v_{ij} \Delta t \tag{8}$$

(3) The grid properties are updated by linearly distributing the properties carried by the particles on to the grid. The grid properties of mass, momentum and energy can be calculated from the individual particle mass (m_P), velocity (v_P) and internal energy (ε_P) with:

$$m_i = \sum_P m_P W_{Pi} \tag{9}$$

$$p_i = \sum_P m_P v_P W_{Pi} \tag{10}$$

$$E_i = \sum_P m_P W_{Pi} \left(\frac{1}{2} v_P^2 + \varepsilon_P \right) \tag{11}$$

The macroscopic equilibrium temperature, T_i, is calculated in each cell in the manner used by conventional finite volume solvers:

$$T_i = \frac{1}{C_v} \left(\frac{E_i}{m_i} - \frac{1}{2} \left(\frac{p_i}{m_i} \right)^2 \right) \tag{12}$$

where C_v is the specific heat under constant volume ($C_v = R(\gamma - 1)^{-1}$). Other macroscopic fluid quantities can be calculated from these values. The linear weights W_{Pi} for each particle are calculated assuming uniform conditions across each cell by:

$$W_{Pi} = \begin{cases} (x_P - x_{i-1})/(x_i - x_{i-1}) & \text{if } x_{i-1} < x_P \leqslant x_i \\ (x_{i+1} - x_P)/(x_{i+1} - x_i) & \text{if } x_i < x_P \leqslant x_{i+1} \\ 0 & \text{otherwise} \end{cases} \tag{13}$$

This linear interpolation scheme is the mathematical representation of the assumption that each particle represents a very large number of particles with identical velocities uniformly distributed across the source cell. Such a scheme is inherently first-order accurate in space. The interpolation routine implemented by Albright in the original QDS does no more than effectively replace the free flight phases of molecular motion which is an assumption present in many modern kinetic theory based flow solvers. The introduction of a higher order interpolation scheme on data which is linearly varying (in space, in this instance) will, at best, perform no better than a linearly interpolating scheme. In addition, no information regarding gradients of conserved or primitive variables appears in either linear or higher order interpolation routines.

2.2. Extension to a second-order scheme

In order to extend the scheme to high order accuracy in a more conventional fashion, the estimates of flux values are improved by adjusting the particle mass, velocity and internal energy in Eqs. (5)–(7) by considering the gradient values calculated at the previous time step using a second-order flux reconstruction scheme. Thus, as an example, the particle mass becomes:

$$m_{ij} = \frac{\left(\rho_i + \frac{d\rho}{dx}\Delta x_L\right)\Delta x w_j}{\sqrt{\pi}} \tag{14}$$

where Δx_L represents the location in the cell from where the flow properties are taken.

This is demonstrated in Fig. 1 showing the addition of a linear variation of density within a cell. Since QDS is essentially a direction coupled volume-to-volume solver, conditions within a region of space are required. Particles moving to a region right of the source cell are likely to have their properties defined by a region in the right half of the cell. In the present implementation, fluxes moving to the right are assumed to take their quantities from the reconstructed state $\Delta x_L = 0.5(\Delta x - v_{ij}dt)$ to the right of the cell center. This corresponds to the centre of mass of the flux which moves into the destination cell. Left moving fluxes have properties constructed in a similar fashion. Particles are then moved in free flight, justifying the use of a linear interpolation routine.

To prevent unphysical and unstable oscillations in the solution, the gradients are calculated using slope limiters. In this scheme, gradients are first determined using the MINMOD (Minimum Modulus) and the MC (Monotonized Central Difference) scheme [14]. Using density as an example, the gradient using the MC slope limiter is:

$$\frac{d\rho}{dx} = \text{MINMOD}\left[\frac{\rho_{i+1} - \rho_{i-1}}{2\Delta x}, \text{MINMOD}\left(2\frac{\rho_{i+1} - \rho_i}{\Delta x}, 2\frac{\rho_i - \rho_{i-1}}{\Delta x}\right)\right] \tag{15}$$

where the MINMOD scheme is:

$$\text{MINMOD}[a,b] = \begin{cases} 0 & \text{IF } (\text{SIGN}(ab) < 0 \\ a & \text{IF } (\text{SIGN}(ab) > 0) \text{ AND } (|a| < |b|) \\ b & \text{IF}(\text{SIGN}(ab) > 0) \text{ AND } (|b| < |a|) \end{cases}$$

2.3. Extension to a higher order finite volume flux scheme

The extension of the scheme to two-dimensions is relatively straight-forward; however, at this stage it becomes convenient to move away from the concept of a particle whose properties are interpolated onto a grid towards a conventional finite volume approach. In this approach, conserved quantities such as mass, momentum and energy are exactly conserved by tracking fluxes from source volumes to destination volumes. Discrete simulation particles are now considered as a very large number of smaller particles uniformly (or linearly) distributed over the source cell. If the particle position distributions (i.e gradients of density in the flow) are known, the flux from the source region to any arbitrary destination volume can be calculated. This concept is illustrated in Fig. 2 for a 2D case. The amount of mass, momentum and energy moving from the source to the destination cell is proportional to the ratio of the area (or volume for 3D) of the overlap to the area of the original cell. This scheme requires minimal computation, works between arbitrarily sized source and destination cells (which makes in suitable for adaptive mesh refinement). Using this concept, the particle mass and velocities in Eqs. (5) and (6) become:

$$m_{ijk} = \frac{\rho_i \Delta x \Delta y w_j w_k}{\pi} \tag{16}$$

$$v_{ij} = u_x + \sqrt{2\sigma_{vi}^2} q_j \tag{17}$$

$$v_{ik} = u_y + \sqrt{2\sigma_{vi}^2} q_k \tag{18}$$

where there are $k = 1,\ldots,K$ particles in the y-coordinate direction.

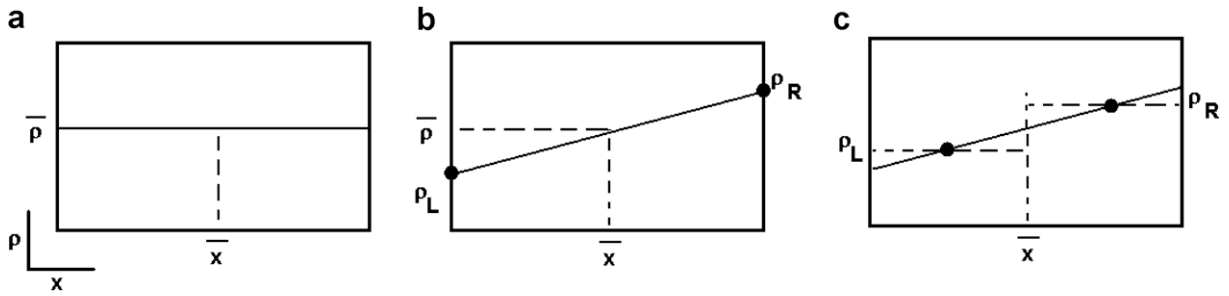

Fig. 1. Examples of addition of in-cell gradients. (a) No gradient, conventional first-order scheme and (b) conventional finite volume implementation where fluxes are calculated at cell interfaces and (c) implementation when calculated fluxes are volume to volume (direction decoupled) as opposed to calculated at flux interfaces.

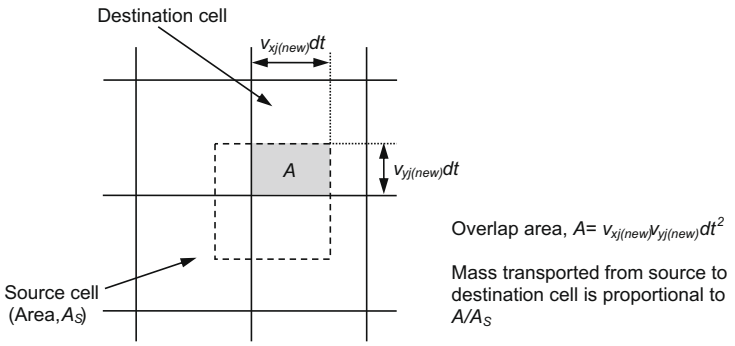

Fig. 2. Schematic showing the way fluxes of conserved quantities between source and destination cells are calculated using the "overlap" function in QDS.

The internal energy remains identical to the one-dimensional case, allowing for a corresponding increase in Ω to account for the extra simulated dimension.

As shown in Fig. 2, the fraction of mass from the source cell which fluxes to the destination cell can be determined by the overlap area $A = v_{xj(new)}v_{yj(new)}dt^2$ divided by the source cell area $dxdy$ for the 2D case. Thus the amount of mass m_{flux}, energy E_{flux} and momentum in each coordinate direction $p_{x,flux}$ and $p_{y,flux}$ which must be added to the destination cell and subtracted from the source cell are given by:

$$m_{flux} = \frac{A}{A_S} m_{ijk} \tag{19}$$

$$E_{flux} = \frac{A}{A_S} m_{ijk} \left[\frac{1}{2} \left(v_{ij}^2 + v_{ik}^2 \right) + \varepsilon_{ijk} \right] \tag{20}$$

$$p_{flux,x} = \frac{A}{A_S} m_{ijk} v_{ij} \tag{21}$$

$$p_{flux,y} = \frac{A}{A_S} m_{ijk} v_{ik} \tag{22}$$

The simulation time step Δt can be set by ensuring the kinetic Courant–Friedrichs–Lewy (CFL) number is maintained at below unity. The kinetic CFL number is given by:

$$\mathrm{CFL} = \frac{\left(|u_i| + q_{j(\max)} \sqrt{RT_i} \right) \Delta t}{\Delta x} \tag{23}$$

where $q_{j(\max)}$ is the maximum value of the particle abscissas (i.e. the value which gives the maximum particle thermal velocity). Thus, the simulation time step is dependent only on the simulation cell size since, in an Euler solver, the mean free path is meaningless since a particle is considered to undergo a theoretically infinite number of collisions at each time step thus bringing it back into perfect thermal equilibrium. Setting the kinetic CFL number ensures that particles are prevented from passing through adjacent cells without undergoing collisions. As long as the kinetic CFL number remains less than one, the influence of CFL on the results is negligible. This is discussed in further detail in the results section.

In the current implementation boundary conditions are handled using ghost cells. These cells can be used to represent walls and inflow or outflow boundaries. The interaction of a gas with a wall is identical to the interaction of that flow with an adjacent cell having the same flow properties but a reversed flow direction. For the inflow boundaries, the ghost cells have properties equal to the free stream conditions, whereas the conditions in outflow ghost cells are interpolated from values within the adjacent flow field cells. In both cases, fluxes from flow field cells to inflow/outflow ghost cells are destroyed.

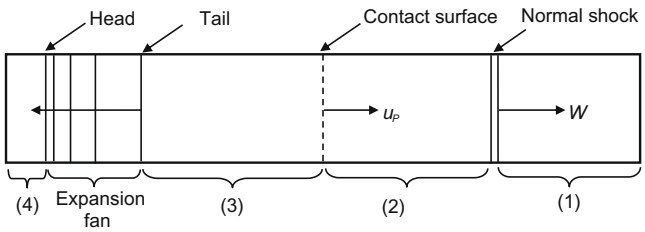

Fig. 3. Flow structure in a shock tube. The flow regions include (1) the undisturbed low-pressure gas, (2) the constant velocity gas behind the shock front, (3) the gas behind the contact surface between the driving and driven gases and (4) the undisturbed high-pressure gas.

3. Code validation

3.1. Shock tube flow

As a validation of the accuracy of the QDS code, we have used the test problem of shock tube flow. Fig. 3 shows the typical flow structure in a shock tube, in which a shock wave is created by bursting a diaphragm between a high-pressure and low-pressure gas. The Riemann analytical continuum solution for a shock tube allows the properties of the flow structure, including the shock propagation velocity W, the contact surface velocity u_P along with the pressure, temperature and density, to be determined at any given time:

$$W = a_1\sqrt{\frac{\gamma+1}{2\gamma}\left(\frac{p_2}{p_1}-1\right)+1} \tag{24}$$

$$u_P = \frac{a_1}{\gamma}\left(\frac{p_2}{p_1}-1\right)\sqrt{\frac{\frac{2\gamma}{\gamma+1}}{\frac{p_2}{p_1}+\frac{\gamma-1}{\gamma+1}}} \tag{25}$$

$$\frac{p_4}{p_1} = \frac{p_2}{p_1}\left[1-\frac{(\gamma-1)(a_1/a_4)(p_2/p_1-1)}{\sqrt{2\gamma\{2\gamma+(\gamma+1)(p_2/p_1-1)\}}}\right]^{-2\gamma/(\gamma-1)} \tag{26}$$

$$\frac{p_3}{p_4} = \left(\frac{p_3}{p_1}\right)\left(\frac{p_1}{p_4}\right) = \left(\frac{p_2}{p_1}\right)\left(\frac{p_1}{p_4}\right) = \left(\frac{\rho_3}{\rho_4}\right)^{\gamma} = \left(\frac{T_3}{T_4}\right)^{\gamma/(\gamma-1)} \tag{27}$$

where a_x, p_x, ρ_x and T_x are respectively the speed of sound, pressure, density and temperature in the region x and γ is the ratio of specific heats.

The simulations were conducted on a one-dimensional shock tube using an ideal monatomic gas. The end walls were simulated as reflective walls. The initial conditions in the high-pressure and low-pressure ends of the shock tube are $p_4 = 10p_1$ and the temperatures at both ends of the tube are the same. This results in a shock Mach number of 1.55. The simulations were carried out using both first- and second-order QDS methods and a first-order TDEFM method. TDEFM is equivalent to QDS (in first-order space and time) in the limit of an infinite number of particles; however, like QDS, TDEFM cannot be considered a benchmark solution because of its inherent numerical diffusion.

Here the simulations QDS utilize three particles per cell and 1000 equi-sized cells. The TDEFM simulation also used 1000 cells. Fig. 4 shows the normalized density $(\rho-\rho_1)/(\rho_4-\rho_1)$ profiles of the shock tube flow after non-dimensional time $t(RT)^{1/2}/L = 0.0686$, while Fig. 5 shows the normalized temperature T/T_1. As can be seen the first-order QDS and TDEFM solutions are essentially equivalent and so possess approximately the same amount of numerical diffusion. The mean percentage difference between the two results over the entire computational domain was 0.13% for density. If the number of particles in QDS is increased, this value reduces (e.g. to 0.06% with 15 particles per cell); however three particles per cells provides sufficient accuracy and low computational expense compared to TDEFM. The second-order QDS result shows reduced numerical diffusion in the region of the shock and contact surface using the same number of particles and cells. The additional computational expense associated with the determination of in-cell gradients for the second-order scheme is less than 5%.

Fig. 6 shows the effect of varying the CFL number on the solution. In this simulation, the maximum CFL is determined at each time step, and the time step adjusted to maintain a constant maximum CFL number during the simulation. The value of the CFL number has little effect on the solution; however some numerical instability is evident in the shock with CFL = 1.0 as

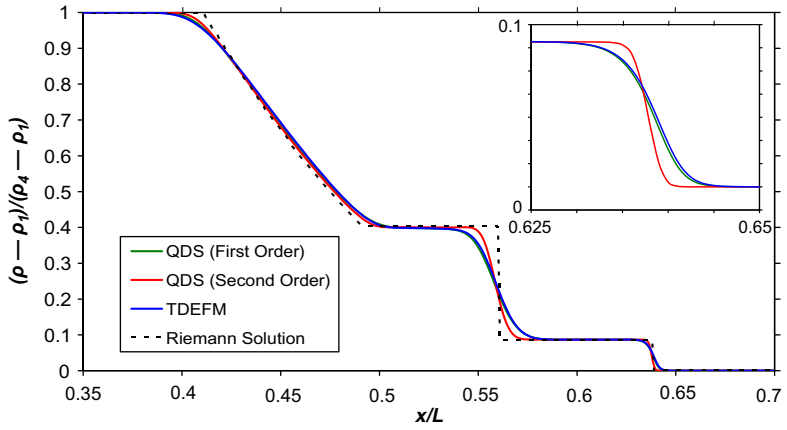

Fig. 4. Shock tube density profile as generated by QDS (first and second-order) and TDEFM compared to the Riemann solution. The inset shows the profile in the region of the shock.

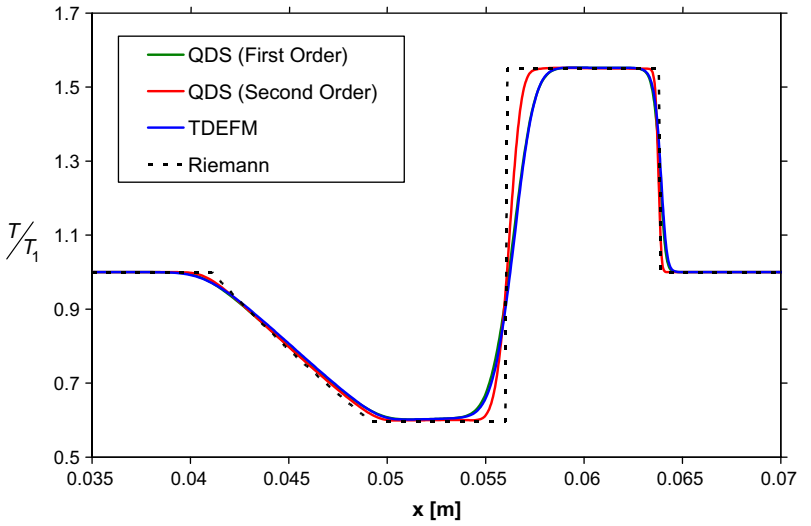

Fig. 5. Shock tube temperature profile as generated by QDS (first- and second-order) and TDEFM compared to the Riemann solution.

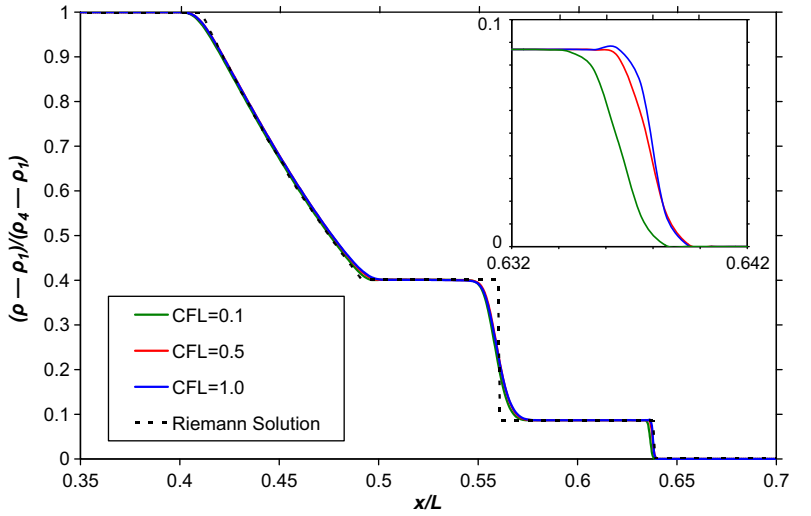

Fig. 6. Shock tube density profile as generated by second-order QDS showing the effect of varying CFL number (via time step variation) on the solution. The inset shows the profile in the region of the shock.

this is the maximum value for which the QDS algorithm used in these simulations remains valid. For CFL > 1.0 fluxes are able to traverse neighbouring cells without interacting. The small difference in shock position is due to the total flow time differing slightly due to the variable time step scheme. Maximising the CFL number (while maintaining maximum CFL < 1.0) decreases the computational expense of the simulations with no loss in accuracy.

Fig. 7 shows the effect cell size at a constant CFL number of 0.5. The solver maintains its stability and predicts accurate positions for the flow features even with large cells; however using smaller cells results in a more accurate solution. The number of cells should therefore be maximised to obtain the most accurate results.

3.2. Two-dimensional blast wave simulation

The second test problem for QDS was the simulation of a two-dimensional circular blast wave. The same problem was used by Smith [5] to demonstrate errors resulting from direction decoupling. As an initial condition, the flow inside a square region of length L is uniform and stationary. The gas is ideal with $\gamma = 1.4$. At zero time, a high temperature gas at 1000 times the ambient temperature is released from a region of radius $0.02L$ at the centre of the domain. The flow was simulated using first- and second-order QDS solvers on a 50×50 grid, along with a Riemann solver and typical results of the density distri-

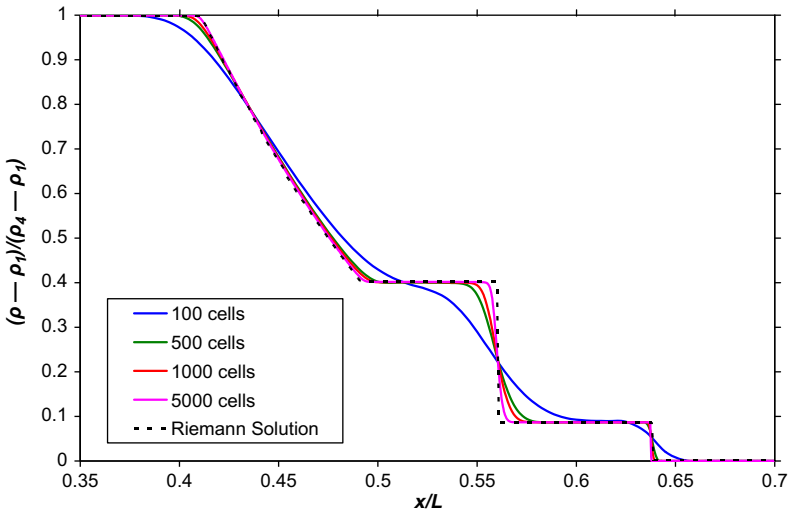

Fig. 7. Shock tube density profile as generated by second order QDS at constant CFL = 0.5 showing the effect of the number of cells on the solution.

bution at some instant are shown in Fig. 8. The computational expense of QDS (first-order) is approximately 10% faster than the Riemann solver, with only a slight increase in the computational expense for extension to second-order. The results demonstrate two of the strengths of QDS. Firstly, the QDS results are far more symmetrical than the Riemann results, since QDS is a direction coupled solver whereas the Riemann solver is not. Secondly, QDS is able to handle a large range in temperatures within the same computational domain (in this case a temperature ratio of 1000 across the blast) while remaining accurate. The large dynamic range and direction coupled nature of the solver are two of the most attractive features of the QDS algorithm. The first-order results obtained using QDS and the Riemann solver force the propagation of the blast front at an artificially high rate due to the uniform distribution of fluxed quantities at each time step. The second order results obtained using QDS much more accurately capture the movement of the blast front, in terms of both location and radial symmetry. The results show that the second-order scheme QDS scheme outperforms both the first-order QDS scheme and the Riemann solver with only a minimal increase of computational cost.

3.3. Mach 3 flow over a forward facing step

The third test problem for the second-order QDS schemes is the Mach 3 flow over a forward facing step in a high speed wind tunnel. This problem was first introduced by Emery [15] and has since been used by Woodward and Colella to test a number of differencing schemes [16]. Fig. 9 shows the geometry and boundary conditions used in the problem. As an initial condition, the flow is everywhere uniform at Mach 3 with a density of 1.4, a pressure of 1.0, gas constant $R = 1.0$ and a spe-

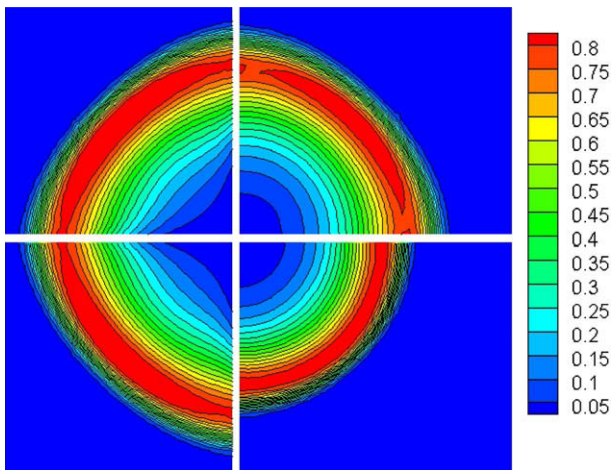

Fig. 8. Contours of density obtained using [left] a first-order accurate Reimann solver, [upper right] first-order QDS and [lower right] second-order QDS for a two-dimensional blast wave on a 50×50 grid.

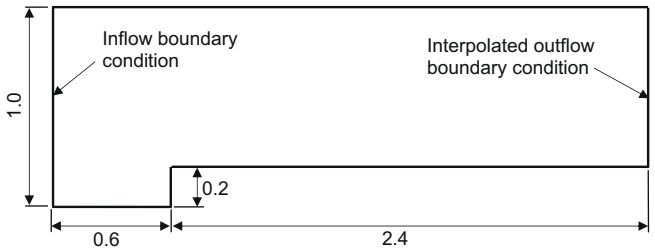

Fig. 9. Geometry and boundary conditions for the Mach 3 flow over a forward facing step in a wind tunnel. All boundaries with exceptions to the inflow and outflow are specularly reflective. The outflow boundary is calculated through interpolation of states of interior cells.

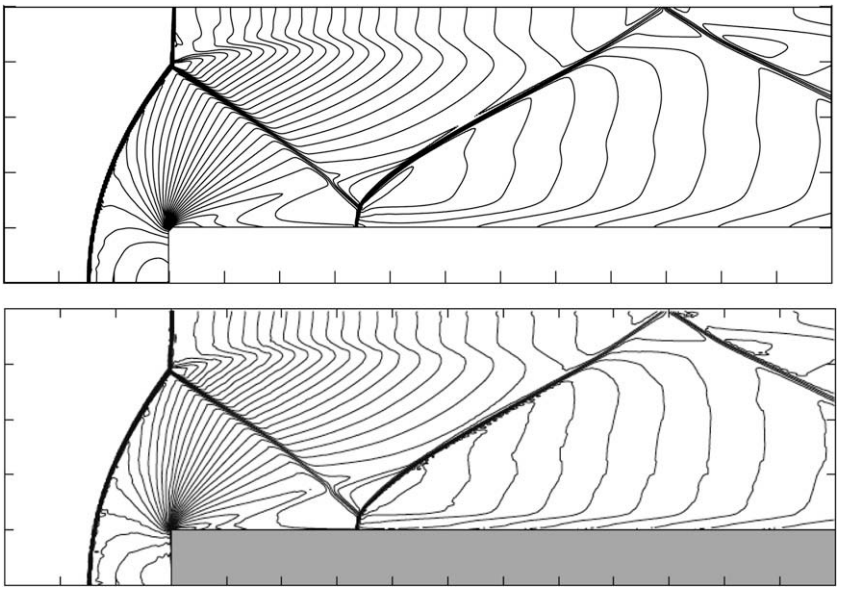

Fig. 10. Contour of density at 4.0 s for Mach 3 flow over a forward facing step in a wind tunnel obtained using second-order QDS with 4 simulation particles (top) and from the results of Keats and Lien [17].

cific heat ratio, $\gamma = 1.4$. This is equivalent to an impulsively started flow and the simulations capture the unsteady development of the flow structure.

The QDS simulations utilized a second-order scheme with 4 particles per cell on a uniform grid consisting of 100,800 square cells. The simulation time step was 0.0005 s. Fig. 10 shows the density profile generated using the QDS solver after 4.0 s (8000 time steps). The result is compared to that of Keats and Lien who employed a second order Godunov method on an adaptively refined mesh [17]. Figs. 11 and 12 show contours of density and temperature respectively in 0.5 s intervals as generated using the second-order QDS solver.

Figs. 10–12 inclusive show that QDS effectively captures all features of the flow field and that the results compare very closely with Keats and Lien's Godunov scheme. The simulations were carried out on a single laptop computer with dual core T2250 Intel processors, and 2 Gb of RAM. To compute 4.0 s of flow required 65 min using the second order QDS solver. By comparison, the same simulation using second-order TDEFM required 201 min. A second-order Riemann solver required 77 min.

Of particular interest is the fact that the QDS solution does not show any evidence of the carbuncle phenomenon which occurs using other finite volume schemes. The carbuncle phenomenon results in a bulge in the stagnation region and a disruption in the shape of the bow shock or unstable and unpredictable variations in density in the stagnation region. The carbuncle phenomenon is not exhibited in the present results, possibly due to the direction coupled nature of QDS and its inherent numerical dissipation, although this may require further investigation.

4. Application – QUIETWAVE blast simulations

The simulation of blast waves has a number of important applications including in the mining industry, in industries which handle dangerous chemicals and gases, and in assessing and countering terrorist threats [18,19]. CFD simulation of

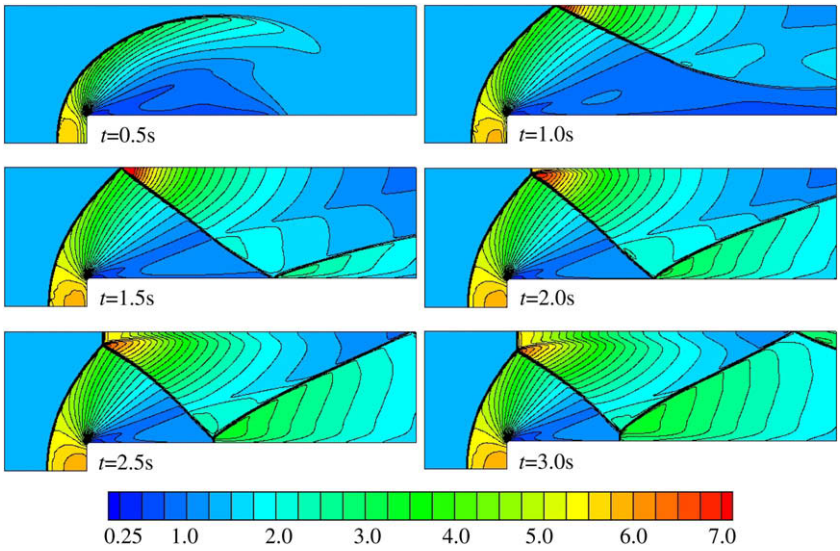

Fig. 11. Contours of density obtained second-order QDS using 4 simulation particles for Mach 3 flow over a forward facing step in a wind tunnel.

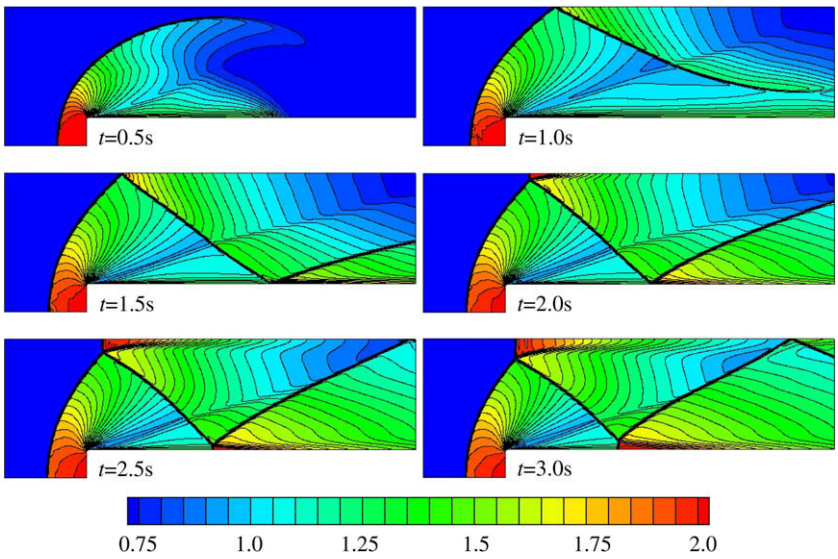

Fig. 12. Contours of temperature obtained using second-order QDS using 4 simulation particles for Mach 3 flow over a forward facing step in a wind tunnel.

blast waves in particular environments is typically a time consuming task requiring an expert user who must design an appropriate grid, set boundary and initial conditions, and select an appropriate solver. A fast and simple solver called FASTWAVE which utilizes the TDEFM method was first proposed by Smith as a tool which can be used by a non-expert user to assess blast-wave scenarios where there is an immediate threat or in an emergency situation. Here the user simply enters the flow field geometry and blast conditions, then the code automatically generates a single block Cartesian grid, boundary and wall conditions are detected automatically and the flow is solved using either Pullin's EFM, Jacobs approximate Riemann solver [20], Macrossan's PFM, or Smith's TDEFM. Recent implementations of FASTWAVE include the modeling of debris, such as broken glass, within the flow, which will be reported elsewhere.

In a test case detailed in Smith's thesis [21], an expert user using CFD-FASTRAN required 82 min to set up and solve a blast wave problem in an arbitrary urban environment, including 28 min solution time. FASTWAVE required 3.5 min, including 2 min of solution time. Although this is a somewhat subjective test, it demonstrates that properly developed tools like FASTWAVE may be useful in emergency and threat situations where the effects of a blast wave need to be predicted rapidly and efficiently.

As demonstrated previously, the QDS method is approximately three times faster than TDEFM for the forward facing step test case. A modified version of FASTWAVE utilizing second-order QDS, called QUIETWAVE, was implemented. Here the TDEFM flux calculation routines were simply replaced by the second-order QDS methods described above.

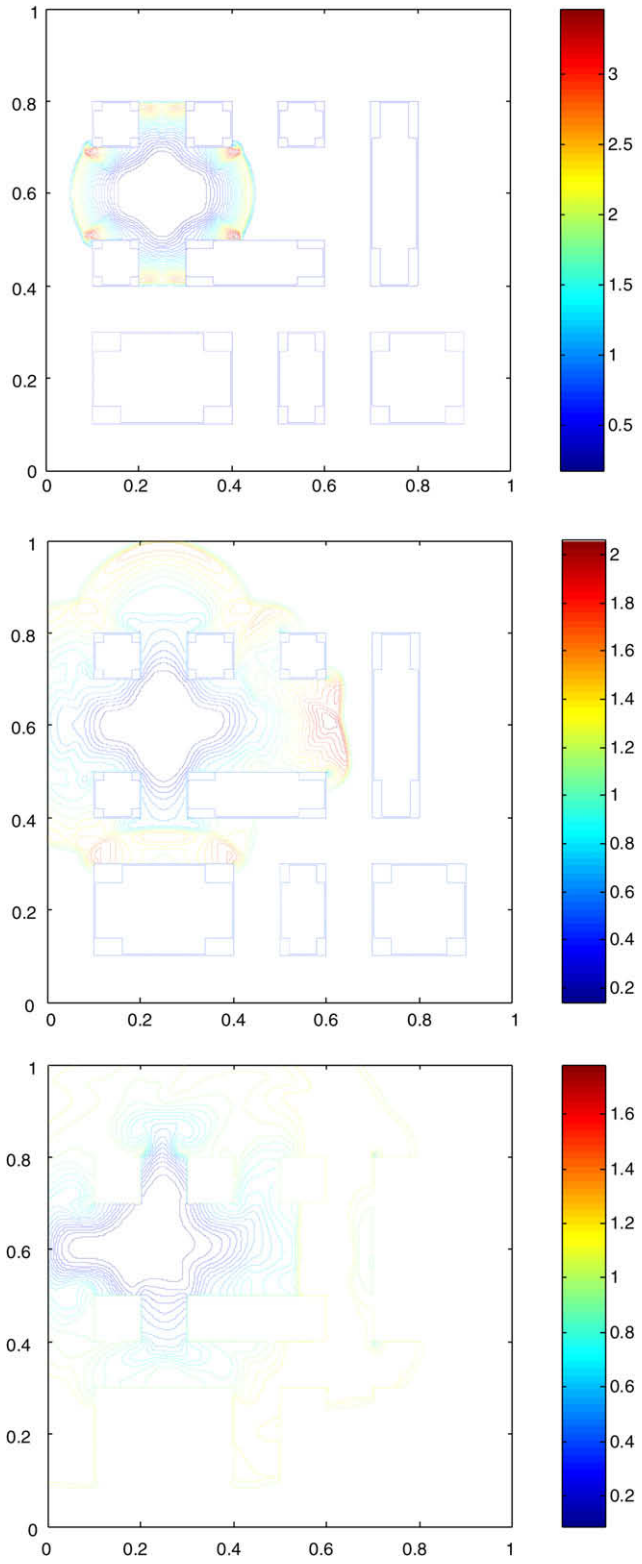

Fig. 13. Contours of density for a blast wave in an urban environment as calculated using QUIETWAVE. Top: at 0.05 s, middle: at 0.15 s and bottom: at 0.25 s.

Fig. 13 shows contours of density at various times for a blast wave propagating in an urban environment consisting of nine buildings. As an initial condition, the flow is everywhere uniform and stationary with a density of 1.0, a temperature of 1.0, gas constant $R = 1.0$ and a specific heat ratio, $\gamma = 1.4$. The sides of the domain are of length $L = 1.0$ and is divided into 400×400 square cells. At zero time, a high temperature gas at 1000 times the ambient temperature is released from a square volume of size $w/L = 0.05$. Building walls consist of specular boundaries and the domain edge is modeled as an interpolated outflow boundary. The total simulation time (for 0.3 s of flow) on a single laptop computer with dual core T2250 Intel processors and 2 Gb of RAM was 36 min.

The results show that QUIETWAVE can rapidly predict blast data in an urban environment demonstrating that this is a useful tool for predicting blast events. Future versions of QUIETWAVE will include the capacity for modeling debris within the flow which has already been implemented in FASTWAVE. The addition of an extra spatial dimension will enable the prediction of blast waves which includes 3D effects. The addition of the third dimension is trivial and simply requires an extra set of weights and abscissas to account for the extra degree of translational freedom of each QDS particle.

5. Conclusions

In this paper a second-order Quiet Direct Simulation (QDS) method was developed and verified. The method uses a monotonized central differencing scheme to calculate the gradients of flow field macroscopic properties and uses these to refine the particle properties which generate the fluxes between cells. Using a verification study of one-dimensional shock tube flow, the method is shown to be more accurate than first-order schemes. Further verification studies of a two-dimensional blast wave and the Mach 3 flow over a forward facing step are used to illustrate the advantages of the method. These are that it is direction coupled method, has a large dynamic range, is much less computationally expensive than other Euler solvers and is not subject to the carbuncle phenomenon.

A method of simulating blast waves in urban environments called QUIETWAVE which utilizes the second-order QDS algorithm is developed. This method yields fast predictions for blast wave behavior in environments with complex geometries and is thus a useful tool for number of important applications including for industries which handle dangerous chemicals and gases, and in assessing and countering terrorist threats.

Acknowledgment

We would like to thank the New Zealand Foundation for Research, Science and Technology (FRST) International Investment Opportunity Fund (IIOF) for the financial support of the second author, Dr. Hadley Cave and the National Science Council of Taiwan for the support of the corresponding author, Prof. J.-S. Wu, through Grant No. 96-2628-E-009-136-MY3.

References

[1] G.A. Bird, Molecular Gas Dynamics and the Direct Simulation of Gas Flows, Clarendon Press, Oxford, 1994.
[2] T.I. Gombosi, Gaskinetic Theory, Cambridge University Press, Cambridge, 1994.
[3] D.I. Pullin, Direct simulation methods for compressible ideal gas flow, J. Comput. Phys. 34 (1980) 231.
[4] M.N. Macrossan, The equilibrium flux method for the calculation of flows with non-equilibrium chemical reactions, J. Comput. Phys. 80 (1989) 204.
[5] M.R. Smith, M.N. Macrossan, M.M. Abdel-jawad, Effects of direction decoupling in flux calculation in finite volume solvers, J. Comput. Phys. 227 (8) (2008) 4142.
[6] B.J. Albright, D.S. Lemons, M.E. Jones, D. Winske, Quiet direct simulation of Eulerian fluids, Phys. Rev. E 65 (2002) 1.
[7] W. Peter, Quiet Direct Simulation Monte Carlo with random time steps, J. Comput. Phys. 221 (1) (2007) 1.
[8] M.N. Macrossan, A particle only hybrid method for near continuum flows, in: Proceedings of 22nd International Symposium on Rarefied Gas Dynamics, vol. 585, 2001, p. 426.
[9] W.F. Chen, Study of hybrid DSMC/EPSM method, Chin. J. Comput. Phys. 20 (3) (2003) 274.
[10] M.R. Smith, Hybrid methods in near-continuum flows, M.Phil. Thesis, University of Queensland, Australia, 2003.
[11] M.G. Wu, Study on hybrid EPSM/EPSM method for chemical reacting flow, Chin. J. Comput. Phys. 20 (3) (2003) 564.
[12] G. Cook, High accuracy capture of curved shock fronts using the method of space-time conservation element and solution element, in: Proceedings of 37th AIAA Aerospace Sciences Meeting and Exhibit, 1998.
[13] W.H. Beyer, CRC Standard Mathematical Tables, CRC Press, Boca Raton (FL), 1987.
[14] B. van Leer, Towards the ultimate conservative difference scheme III: Upstream centered finite difference schemes for ideal compressible flow, J. Comput. Phys. 23 (1977) 263.
[15] A.E. Emery, An evaluation of several differencing methods for inviscid fluid problem, J. Comput. Phys. 2 (1968) 306.
[16] P. Woodward, P. Collela, The numerical simulation of two-dimensional fluid flow with strong shocks, J. Comput. Phys. 54 (1984) 115.
[17] W.A. Keats, F.S. Lien, Two-dimensional anisotropic cartesian mesh adaptation for the Euler Equations, Int. J. Numer. Meth. Eng. 46 (2004) 1099.
[18] P.D. Smith, T.A. Rose, Blast wave propagation in city streets – an overview, Progr. Struct. Eng. Mater. 8 (2006) 16.
[19] P.D. Smith, G.P. Whalen, L.J. Feng, T.A. Rose, Blast loading on buildings from explosions in city streets, Proc. Inst. Civil Eng. Struct. Build. J. 146 (1) (2001) 47.
[20] P.A. Jacobs, MBCNS: a computer program for the simulation of transient compressible flows, Department of Mechanical Engineering Report 7/98, The University of Queensland, Australia, 1998.
[21] M.R. Smith, The true direction equilibrium flux method and its application, PhD Thesis, University of Queensland, Australia, 2008.